

Original citation:

Dias, F. T., Vieira, V. N., Garcia, E. L., Wolff-Fabris, F., Kampert, Erik, Gouvêa, C .P., Schaf, J., Obradors, X., Puig, T. and Roa, J. J.. (2016) Functional behavior of the anomalous magnetic relaxation observed in melt-textured YBa₂Cu₃O_{7-δ} samples showing the paramagnetic Meissner effect. *Physica C: Superconductivity and its Applications*, 529 . pp. 44-49.

Permanent WRAP URL:

<http://wrap.warwick.ac.uk/87956>

Copyright and reuse:

The Warwick Research Archive Portal (WRAP) makes this work by researchers of the University of Warwick available open access under the following conditions. Copyright © and all moral rights to the version of the paper presented here belong to the individual author(s) and/or other copyright owners. To the extent reasonable and practicable the material made available in WRAP has been checked for eligibility before being made available.

Copies of full items can be used for personal research or study, educational, or not-for-profit purposes without prior permission or charge. Provided that the authors, title and full bibliographic details are credited, a hyperlink and/or URL is given for the original metadata page and the content is not changed in any way.

Publisher's statement:

© 2016, Elsevier. Licensed under the Creative Commons Attribution-NonCommercial-NoDerivatives 4.0 International <http://creativecommons.org/licenses/by-nc-nd/4.0/>

A note on versions:

The version presented here may differ from the published version or, version of record, if you wish to cite this item you are advised to consult the publisher's version. Please see the 'permanent WRAP url' above for details on accessing the published version and note that access may require a subscription.

For more information, please contact the WRAP Team at: wrap@warwick.ac.uk

Functional behavior of the anomalous magnetic relaxation observed in melt-textured $\text{YBa}_2\text{Cu}_3\text{O}_{7-\delta}$ samples showing the paramagnetic Meissner effect

F.T. Dias^{a,*}, V.N. Vieira^a, E. L. Garcia^a

^a*Instituto de Física e Matemática, Universidade Federal de Pelotas, Caixa Postal 354, 96010-900, Pelotas, Rio Grande do Sul, Brazil*

F. Wolff-Fabris^b, E. Kampert^b

^b*Dresden High Magnetic Field Laboratory, Helmholtz-Zentrum Dresden-Rossendorf, 01314, Dresden, Germany*

C.P. Gouvêa^c

^c*National Institute of Metrology, Quality and Technology (Inmetro), Material Metrology Division, 25250-020, Duque de Caxias, Rio de Janeiro, Brazil*

J. Schaf^d

^d*Instituto de Física, Universidade Federal do Rio Grande do Sul, 91501-970, Porto Alegre, Rio Grande do Sul, Brazil*

X. Obradors^e, T. Puig^e

^e*Institut de Ciència de Materials de Barcelona, CSIC, Universitat Autònoma de Barcelona, 08193, Bellaterra, Spain*

J.J. Roa^f

^f*Departamento de Ciencia de Materiales e Ingeniería Metalúrgica, Universitat Politècnica de Catalunya, 08028, Barcelona, Spain*

Corresponding author: F. T. Dias

E-mail address: fabio.dias@ufpel.edu.br

Alternative e-mail: diasft@gmail.com

ABSTRACT

We have studied the functional behavior of the field-cooled (FC) magnetic relaxation observed in melt-textured $\text{YBa}_2\text{Cu}_3\text{O}_{7-\delta}$ (Y123) samples with 30 wt% of $\text{Y}_2\text{Ba}_1\text{Cu}_1\text{O}_5$ (Y211) phase, in order to investigate anomalous paramagnetic moments observed during the experiments. FC magnetic relaxation experiments were performed under controlled conditions, such as cooling rate and temperature. Magnetic fields up to 5T were applied parallel to the ab plane and along the c-axis. Our results are associated with the paramagnetic Meissner effect (PME), characterized by positive moments during FC experiments, and related to the magnetic flux compression into the samples. After different attempts our experimental data could be adequately fitted by an exponential decay function with different relaxation times. We discuss our results suggesting the existence of different and preferential flux dynamics governing the anomalous FC paramagnetic relaxation in different time intervals. This work is one of the first attempts to interpret this controversial effect in a simple analysis of the pinning mechanisms and flux dynamics acting during the time evolution of the magnetic moment. However, the results may be useful to develop models to explain this interesting and still misunderstood feature of the paramagnetic Meissner effect.

Keywords: magnetic relaxation, paramagnetic Meissner effect, magnetic flux dynamics

1. Introduction

The Meissner effect is one of the most important features of the superconducting state, characterized by a diamagnetic response showed by a superconducting material due to exclusion of the magnetic flux from its interior, when the temperature is below the critical temperature (T_C). The effect can be observed during a field-cooled (FC) process, when the sample is cooled under an applied magnetic field. In type-II superconductors a perfect diamagnetism can be observed only when the magnetic applied field is lower than $H_{C1}(T)$, the lower critical field. When the magnetic field is higher than $H_{C1}(T)$ but lower than $H_{C2}(T)$, the upper critical field, the magnetic field penetrate in the form of vortices, and the material exhibits an incomplete Meissner effect.

However, in several situations the superconducting material exhibits a paramagnetic response during a FC process, contrasting with the usual diamagnetic behavior, and the effect is called Paramagnetic Meissner Effect, or simply PME. In the PME the magnetic flux is not expelled, but penetrates into the material creating a paramagnetic state. In some cases the positive magnetic moments can increase with the applied magnetic field in such way that the PME is reinforced with the increase of the magnetic field. Originally the PME was observed in polycrystalline samples of high temperature superconductors [1,2], however, the effect has been observed in several superconducting systems and under different magnetic field ranges [3-18].

A curious and interesting feature is the anomalous time dependence of the FC magnetic moment observed in some superconducting samples [7,13,14,19,20]. This behavior manifests itself as a strong paramagnetic relaxation, contrasting with the expected diamagnetic relaxation. The paramagnetic relaxation generally increases with time and shows dependencies with the magnetic field, temperature and the cooling rate employed [13]. In spite of the numerous efforts to explain the PME [18,21-25], there is not a consistent model to explain the paramagnetic relaxation observed in samples that exhibit the PME.

In this study we report on FC magnetic moment relaxation experiments in two melt-textured $YBa_2Cu_3O_{7-8}$ samples that exhibit the PME and enhanced vortex pinning characteristics. Our goal is present a simple model to describe the functional behavior of the paramagnetic relaxation exhibited by our samples, that can be useful to understand the possible vortex dynamics acting during the time evolution of the PME.

2. Experimental details

2.1. Sample preparation

The two melt-textured $YBa_2Cu_3O_{7-8}$ samples investigated in this work were grown at the Institute of Materials Science of Barcelona, and at the Department of Materials Science and Metallurgical Engineering of the University of Barcelona, Spain. The samples, labeled as MT30-I and MT30-II, were produced by the top-seeding technique. Single crystalline seeds of the $Nd_1Ba_2Cu_3O_{7-8}$ superconductor were placed on top of the $YBa_2Cu_3O_{7-8}$ pellets to induce the crystallographic texture. Both samples were grown starting from pre-sintered ceramic pellets of $YBa_2Cu_3O_{7-8}$ containing 30 wt% of the non-superconducting $Y_2Ba_1Cu_1O_5$ (Y211) phase.

The melt-textured pieces were cut with a diamond saw in small parallelepipeds with 3.0mm in length along the ab plane, 2.1mm in thickness (ab plane) and 2.0mm along the c-axis. The samples were characterized by electron microscopy in order to verify the grain alignment. Fig. 1 shows an image obtained from MT30-I sample using a scanning electron microscope Nova Nanolab 600 from Fei Company, where long platelets (superconducting grains) can be seen along the ab plane, typical of good melt-textured samples.

2.2. Magnetic measurements

The magnetic measurements were performed with a MPMS-XL SQUID magnetometer and a vibrating sample magnetometer (VSM), both from Quantum Design, in magnetic fields up to 5T applied along the *c*-axis and parallel to the *ab* plane. The experimental results were always corrected for temperature gradient and demagnetization effects. Initially the magnetic moments were measured as a function of the temperature according to the zero-field cooling (ZFC) and field-cooled (FC) prescriptions. The ZFC results (not shown here) always showed the usual diamagnetic response, due to shielding effects. The FC measurements were performed with two different procedures namely, field-cooled cooling (FCC) and field-cooled warming (FCW) prescriptions.

In the FCC prescription the magnetic moment was measured while cooling the sample to temperatures below the critical temperature (T_C) in an applied magnetic field. In the FCW prescription, always performed in sequence and immediately after the FCC experiment, the magnetic moment was measured under the same constant magnetic field while the sample warms up to temperatures above T_C .

The FC magnetic moment relaxation experiments were performed at fixed temperature and magnetic field. In this case, similar to FCC prescription, the sample is cooling down to a temperature below T_C , under a constant magnetic field and also under a fixed cooling rate. In sequence the magnetic moment was measured as a function of time in a constant magnetic field and a fixed temperature for long time intervals. Part of the experimental results employed in this study were extracted from our previous works, however, such measurements were analyzed in details and for the first time in the present work.

3. Results and discussion

3.1. FC measurements

The PME in our samples was clearly identified by FC measurements, as shown in Fig. 2, for magnetic fields of 2T and 5T applied along the *ab* plane in the MT30-II sample. For low magnetic fields the magnetic response is diamagnetic, as shown in the inset of the Fig. 2 for a magnetic field of 0.06T. Similar behavior was found for MT30-I sample. Inspecting the Fig. 2, for magnetic fields of 2T and 5T, it is possible to observe irreversibilities among FCC (closed circle) and FCW (open square) measurements. These irreversibilities are stronger for the magnetic field of 2T, as indicated by the arrows, where the FCW magnetic moment is more positive than the FCC magnetic moment. These irreversibilities were also observed in previous works [7,13,17,19], and have been attributed to time effects. For the magnetic field of 0.06T the Meissner effect is conventional (diamagnetic response) and such irreversibilities are inexistent.

In our view the PME results in our samples may be explained in terms of the compression of the magnetic flux, as originally proposed by Koshelev and Larkin [23]. According to this idea, a strong nonequilibrium compressed flux state could be originated and stabilized by an inhomogeneous cooling of the superconducting material below T_C . In this scenario, that can be possible in small samples, and even in single crystals [7,13,14,17], the surface of the material could become superconducting before the bulk and the magnetic flux could be expelled outside or inside the material. As a possible consequence, if the magnetic flux is expelled inside the material it could be pushed into its interior, originating a flux compressed state, that can be stabilized by pinning centers, in our case the Y211 phase. During the magnetic flux compression the sample can admit the entrance of new vortices, increasing the positive moment with time and causing the FCC/FCW irreversibilities. These irreversibilities, as shown in the Fig. 2, are a clear evidence of relaxation processes occurring in our samples. Similar results can be found in the literature [7,13,14,17,20,24]. On the other hand, when low magnetic fields are applied, the magnetic flux compression mechanism is weaker than the conventional Meissner effect, and a diamagnetic moment can be observed, such as shown in the inset of the Fig. 2.

3.2. Paramagnetic relaxation measurements and functional analysis

We performed specific FC magnetic relaxation experiments, according to the experimental procedures described in the section 2.2, in order to investigate the time evolution of the FC magnetic moment in our samples. Some representative results are shown in the Fig. 3.

The Fig. 3 shows three FC magnetic relaxation measurements (open circle), performed under different cooling rates, magnetic fields and temperatures. The Figs. 3a and 3b are representative of the results obtained with MT-I sample, while the Fig. 3c is representative for the MT-II sample. A pronounced paramagnetic relaxation can be observed in all experiments, increasing with time and with no apparent tendency to saturation for long time intervals. Similar results were found in several experimental situations (not shown here) for both samples, varying the cooling rate, magnetic field and temperature.

The results shown in the Fig. 3 are not new in the literature, and have been reported in previous works [7,13,14,19]. They may be interpreted as the admission of extra magnetic flux into the sample as a consequence of the magnetic flux mechanism at fixed temperatures [13], as discussed in the section 3.1. This anomalous behavior is the opposite to the expectations based on the flux-creep model [26].

In order to understand the functional behavior of the magnetic relaxation shown in the Fig. 3, and the vortex dynamics acting during the process, we proceeded some tentatives to fit the experimental data. An initial and obvious choice was a simple exponential function, like $M = Ae^{-t/t_0}$, however, the results were not satisfactory. The other choice was a double exponential function,

$$(1) \quad M(t) = M_0 + A_1e^{-t/t_1} + A_2e^{-t/t_2} ,$$

where $M(t)$ is the magnetic moment, M_0 , A_1 and A_2 are parameters obtained from the adjust, and t_1 and t_2 are the characteristic times. The fitting with the double exponential function proved to be satisfactory and adequate to our experimental data. Some representative results are shown in the Fig. 3, represented by the black solid curve over the experimental data (open circle), with the characteristic times specified in each curve. As can be seen in the Fig. 3, there is a clear difference in the order of magnitude among the characteristic times t_1 and t_2 for all results. This behavior apparently indicates the existence of two different mechanisms acting during the relaxation process in our samples.

The combination of two exponential functions allowed us to define the time intervals of the dominance of each one in the Eq. (1). Consequently we performed a separate fitting in order to estimate these limits. The results are shown in the Fig. 4, for the same measurements presented in the Fig. 3. In this case the function adopted was

$$(2) \quad M(t) = M_0 + Ae^{-t/T} ,$$

where $M(t)$ is the magnetic moment, M_0 and A are parameters obtained from the adjust, and T is the characteristic time. The two black solid curves over the experimental data represent the fitting with (2) for each curve. Obviously the fitting quality in this case are not the same that the Fig. 3, due to splitting in two independent exponential functions. However, the Fig. 4 shows, for the three measurements, an exponential function that quickly saturates in the early stages of the relaxation process, followed by an exponential function that dominates the subsequent time interval.

In our view, the results presented in the Figs. 3 and 4 may be explained assuming that this behavior is representative of the existence of two different magnetic flux dynamics responsible for the admission of extra vortices inside the samples. These different magnetic flux dynamics can act in different time intervals, as a consequence of the compression flux scenario due to PME.

In the early stages of the magnetic relaxation the vortices penetrate in the grain junctions (weak

links), configuring a Josephson dynamics scenario. Melt-textured samples are known to have oriented long platelets microstructure, as can be seen in the Fig. 1. As a consequence, such microstructure shows a reduced number of weak links. Therefore, melt-textured materials exhibit a reduced granularity, however, although the number of weak links is reduced in this material, there are spaces among the superconducting grains that allow the entrance of extra vortices. Consequently, the Josephson dynamics is responsible for the fast relaxation observed in the early stages of the relaxation process, followed by a subsequent saturation, as can be seen in the Fig. 4. We believe that the saturation of the magnetic moment is exactly due to reduction in grain junctions, allowing only a limited amount of vortices penetrate into the sample.

On the other hand, the black solid curves fitting the long time intervals in the Fig. 4 may be representative of the Abrikosov dynamics. The Abrikosov dynamics can be characterized by the penetration of vortices into the superconducting platelets in the form of intragrain vortices (Abrikosov vortices), with the subsequent pinning by the Y211 particles dispersed into the grains. This mechanism practically dominates the relaxation process, as can be seen in the three measurements shown in the Fig.4. The two magnetic flux dynamics are indicated in the Fig. 4a. More results are presented in the Fig. 5 for different experimental conditions, corroborating the results presented in the Figs. 3 and 4. The splitting of the magnetic relaxation in two components can be clearly observed for both samples, independent on the cooling rate and the magnetic field employed, configuring the different magnetic flux dynamics proposed, as indicated in the Fig. 5b.

4. Conclusion

We performed an experimental study about the anomalous FC magnetic relaxation in two melt-textured $\text{YBa}_2\text{Cu}_3\text{O}_{7-\delta}$ samples that exhibit the paramagnetic Meissner effect (PME). The purpose of this work is to investigate the functional behavior and consequently the magnetic flux dynamics involved during the relaxation process. We believe that our PME can be described in terms of the flux compression model developed by Koshelev and Larkin [23]. Based on a fitting with a double exponential function, we believe that our experimental data can be governed by two different magnetic flux dynamics, in different time intervals of the relaxation process. In the early stages a Josephson-type dynamics is the dominant mechanism, responsible for the admission of extra vortices among the superconducting grains, reinforcing the flux compression and consequently the establishment of the PME. After the relaxation process is governed by an Abrikosov-type dynamics, with the magnetic flux being moved to inside the superconducting grains and pinned by the Y211 particles dispersed.

Finalizing, our results constitute a simple and interpretative analysis, sometimes speculative, of the FC magnetic relaxation in samples that exhibit the PME. Due to the lacking of works exploring the functional behavior of the magnetic relaxation connected to PME, our results may supply important elements to more detailed models on this interesting effect.

Acknowledgements

This work was financed by the Brazilian MCTI/CNPq Universal 14/2012 (contract number 477506/2012-7). We acknowledge the support of the HLD-HZDR, member of the European Magnetic Field Laboratory (EMFL).

5. References

- [1] P. Svedlinh, K. Niskanen, P. Norling, P. Nordblad, L. Lundgren, B. Lönnberg, T. Lundström, Anti-Meissner effect in the BiSrCaCuO-system, *Physica C* 162–164 (1989) 1365-1366.
- [2] W. Braunisch, N. Knauf, V. Kataev, S. Neuhausen, A. Grütz, A. Kock, B. Roden, D. Khomskii, D. Wohlleben, Paramagnetic Meissner effect in Bi high-temperature superconductors, *Phys. Rev. Lett.* 68 (1992) 1908-1911.
- [3] D. Khomskii, Wohlleben Effect (Paramagnetic Meissner Effect) in High-Temperature superconductors, *J. Low Temp. Phys.* 95 (1994) 205-223.
- [4] S. Riedling, G. Bräuchle, R. Lucht, K. Röhberg, H.v. Löhneysen, H. Claus, A. Erb, G. Müller-Vogt, Observation of the Wohlleben effect in $\text{YBa}_2\text{Cu}_3\text{O}_{7-\delta}$ single crystals, *Phys. Rev. B* 49 (1994) 13283-13286.
- [5] M.S.M. Minhaj, D.J. Thompson, L.E. Wenger, J.T. Chen, Paramagnetic Meissner effect in a niobium disk, *Physica C* 235-240 (1994) 2519-2520.
- [6] D. Brandt, C. Binns, S.J. Gurman, G. Torricelli, D.S.W. Gray, Paramagnetic Meissner Transitions in Pb Films and the Vortex Compression Model, *J. Low Temp. Phys.* 163 (2011) 170-175.
- [7] F.T. Dias, P. Pureur, P. Rodrigues Jr., X. Obradors, Paramagnetic Meissner effect at high fields in melt-textured $\text{YBa}_2\text{Cu}_3\text{O}_{7-\delta}$, *Physica C* 354 (2001) 219-222.
- [8] R. Lucht, H.v. Löhneysen, H. Claus, M. Kläser, G. Müller-Vogt, Surface-sensitive paramagnetic Meissner effect in $\text{YBa}_2\text{Cu}_3\text{O}_x$ single crystals, *Phys. Rev. B* 52 (1995) 9724-9726.
- [9] C. Shaoyan, A.J. Schwartz, T.B. Massalski, D.E. Laughlin, Extrinsic paramagnetic Meissner effect in multiphase indium-tin alloys, *Appl. Phys. Lett.* 89 (2006) 111903 (3pp).
- [10] A.G. Lebed, Paramagnetic intrinsic Meissner effect in layered superconductors, *Phys. Rev. B* 78 (2008) 012506 (4pp).
- [11] M.A.L. de la Torre, V. Peña, Z. Sefrioui, D. Arias, C. Leon, J. Santamaria, J.L. Martinez, Paramagnetic Meissner effect in $\text{YBa}_2\text{Cu}_3\text{O}_7/\text{La}_{0.7}\text{Ca}_{0.3}\text{MnO}_3$ superlattices, *Phys. Rev. B* 73 (2006) 052503 (4pp).
- [12] L. Balicas, G. Li, R.R. Urbano, P. Goswami, C. Tarantini, B. Lv., P. Kuhns, A.P. Reyes, C.W. Chu, Anomalous hysteresis as evidence for a magnetic-field-induced chiral superconducting state in LiFeAs , *Phys. Rev. B* 87 (2013) 024512 (10pp).
- [13] F.T. Dias, P. Pureur, P. Rodrigues Jr., X. Obradors, Paramagnetic effect at low and high magnetic fields in melt-textured $\text{YBa}_2\text{Cu}_3\text{O}_{7-\delta}$, *Phys. Rev. B* 70 (2004) 224519 (9pp).

[14] F.T. Dias, V.N. Vieira, M.L. de Almeida, A.L. Falck, P. Pureur, J.L. Pimentel Jr., X. Obradors, Paramagnetic Meissner effect at high fields in YCaBaCuO single crystal and melt-textured YBaCuO, *Physica C* 470 (2010) S111-S112.

[15] A.I. Rykov, S. Tajima, F.V. Kusmartsev, High-field paramagnetic effect in large crystals of YBa₂Cu₃O_{7-δ}, *Phys. Rev. B* 55 (1997) 8557-8563.

[16] D.A. Luzhbin, A.V. Pan, V.A. Komashko, V.S. Flis, V.M. Pan, S.X. Dou, P. Esquinazi, Origin of paramagnetic magnetization in field-cooled YBa₂Cu₃O_{7-δ} films, *Phys. Rev. B* 69 (2004) 024506 (7pp).

[17] Md. Matin, L.S. Sharath Chandra, M.K. Chattopadhyay, M.N. Singh, A.K. Sinha, S.B. Roy, High field paramagnetic effect in the superconducting state of Ti_{0.8}V_{0.2} alloy, *Supercond. Sci. Technol.* 26 (2013) 115005 (7pp).

[18] A.K. Geim, S.V. Dubonos, J.G.S. Lok, M. Henini, J.C. Maan, Paramagnetic Meissner effect in small superconductors, *Nature* 396 (1998) 144-146.

[19] A. Terentiev, D.B. Watkins, L.E. De Long, D.J. Morgan, J.B. Ketterson, Paramagnetic relaxation and Wohleben effect in field-cooled Nb thin films, *Phys. Rev. B* 60 (1999) R761-R764.

[20] F.T. Dias, V.N. Vieira, D.L. Silva, F. Wolff-Fabris, E. Kampert, M.L. Almeida, F. Mesquita, M. Hneda, J.J. Roa, Paramagnetic moments and time effects in melt-textured NdBaCuO system with Nd422 inclusions, *J. of Phys.: Conf. Series* 592 (2015) 012064 (6pp).

[21] M. Sigrist, T.M. Rice, Unusual paramagnetic phenomena in granular high-temperature superconductors - A consequence of d-wave pairing?, *Rev. Mod. Phys.* 67 (1995) 503-513.

[22] F.V. Kusmartsev, Destruction of the Meissner Effect in Granular High-Temperature Superconductors, *Phys. Rev. Lett.* 69 (1992) 2268-2271.

[23] A.E. Koshelev, A.I. Larkin, Paramagnetic moment in field-cooled superconducting plates: Paramagnetic Meissner effect, *Phys. Rev. B* 52 (1995) 13559-13562.

[24] V.V. Moshchalkov, X.G. Qiu, V. Bruyndoncx, Paramagnetic Meissner effect from the self-consistent solution of the Ginzburg-Landau equations, *Phys. Rev. B* 55 (1997) 11793-11801.

[25] Y.V. Obukhov, The "Paramagnetic" Meissner Effect in Superconductors, *J. Supercond.* 11 (1998) 733-736.

[26] Y. Yeshurun, A.P. Malozemoff, Giant Flux Creep and Irreversibility in an Y-Ba-Cu-O Crystal: An Alternative to the Superconducting-Glass Model, *Phys. Rev. Lett.* 60 (1988) 2202-2205.

Figure captions

Fig. 1. SEM image of the MT30-I sample showing a platelet structure stacked along the c-axis, typical of melt-textured materials.

Fig. 2. FCC (closed circle) and FCW (open square) magnetic moment measurements in the MT30-II sample for magnetic fields of 2T and 5T, applied along the ab plane. Irreversibilities can be observed, as indicated by the arrows. The inset shows the same measurements for a magnetic field of 0.06T. The result for 5T was obtained using a SQUID magnetometer, in the first charging of the magnet (no overshoot) after the whole magnetometer was warmed up to room temperature.

Fig. 3. FC magnetic relaxation measurements (open circle) for the samples MT30-I and MT30-II under different experimental conditions, performed by a vibrating sample magnetometer (VSM). The measurements were obtained for the first charging of the field, after the magnetometer be warmed up to room temperature and cooled again. The black solid lines are fittings with the Eq. (1), with the respective characteristic times indicated for each curve. M_0 is the magnetic moment when $t = 0$ s.

Fig. 4. The splitting of the respective fittings presented in the Fig. 3 using the Eq. (2). The corresponding vortex dynamics for each time interval are indicated in the Fig. a.

Fig. 5. Left side: FC magnetic relaxation measurements performed by a SQUID magnetometer under different experimental conditions for both samples, coupled with fittings from the Eq. (1) and similar to the results presented in the Fig. 3. Similar to results of the Fig. 3, the measurements were obtained for the first charging of the field, after the magnetometer be warmed up to room temperature and cooled again. Right side: The respective splitting from the Eq. (2) with the corresponding vortex dynamics, similar to the results presented in the Fig. 4.

FIGURES

Fig. 1

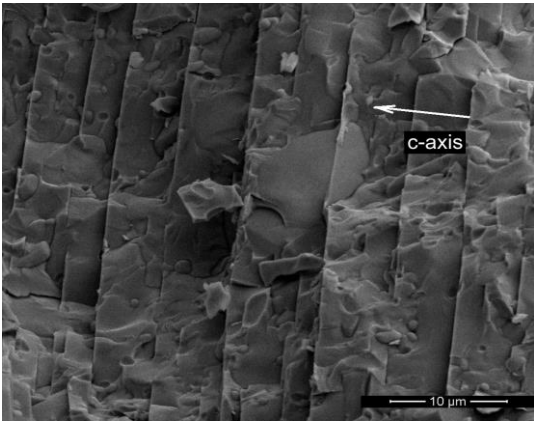


Fig. 2

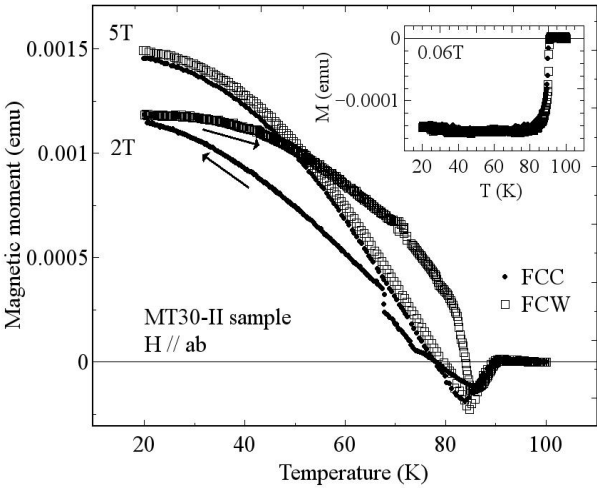


Fig. 3

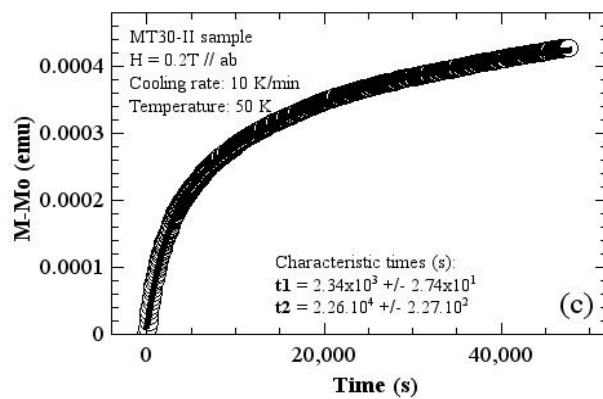
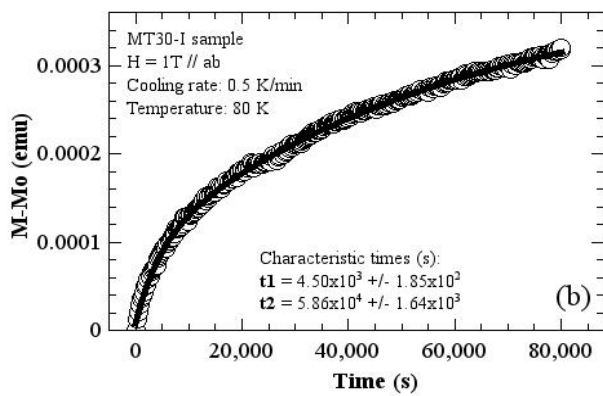
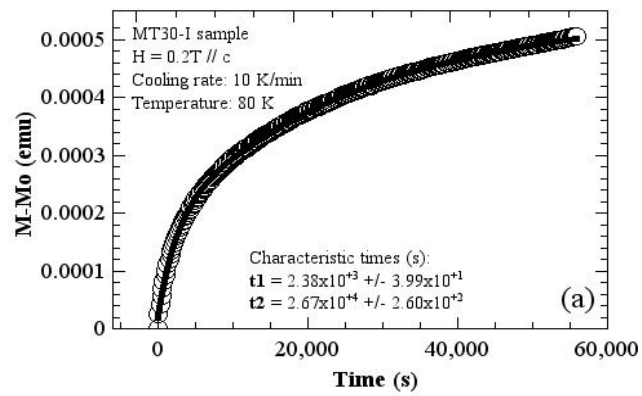


Fig. 4

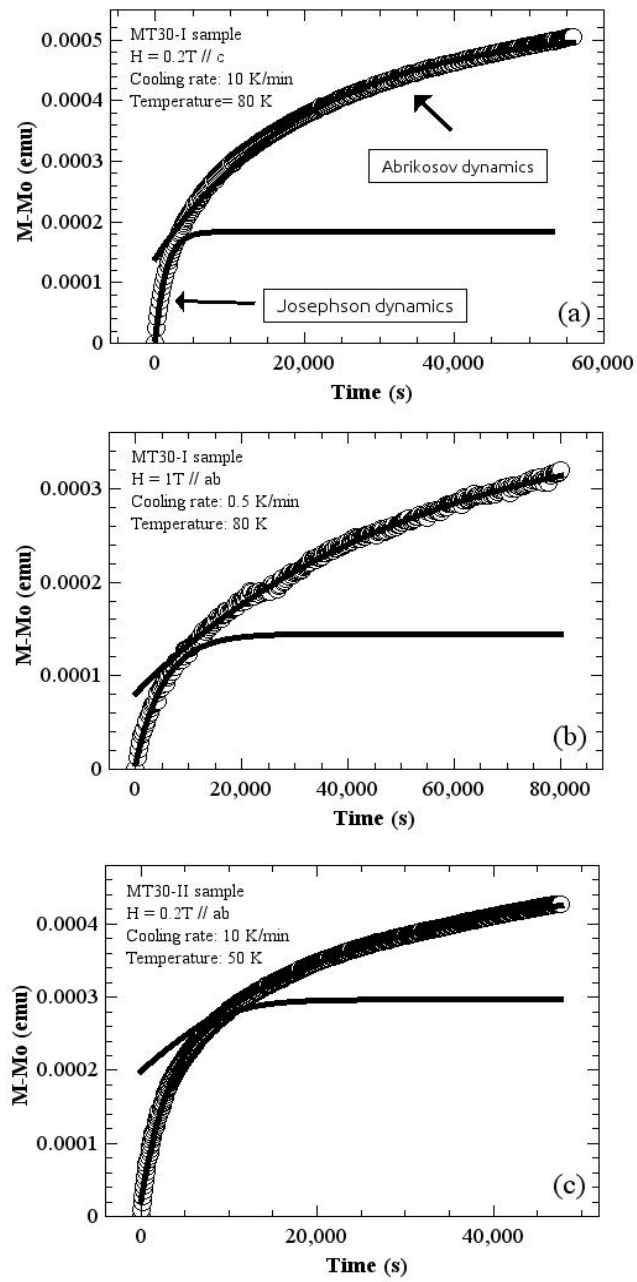


Fig. 5

